Cyano-Bridged Complexes of *trans*-Tetrakis(pyridine)ruthenium(II)

Benjamin J. Coe,*,† Thomas J. Meyer,* and Peter S. White

Department of Chemistry, The University of North Carolina, Chapel Hill, North Carolina 27599-3290

Received November 1, 1994[⊗]

Reaction of *trans*-$[RuCl(py)_4(Me_2CO)]^+$ with cyanide ion produces *trans*-$RuCl_2(py)_4$ and *trans*-$[Ru(OCH_3)_2(py)_4]^+$, but almost no *trans*-$RuCl(CN)(py)_4$. The asymmetrical bimetallic complex salt *trans*-$[Cl(py)_4Ru(NC)Ru(py)_4(CN)]PF_6$ (**1**) was prepared by reaction of *trans*-$[RuCl(py)_4(Me_2CO)]^+$ with an excess of *trans*-$Ru(CN)_2(py)_4$. The symmetrical trimetallic complex salt *trans*-$[Cl(py)_4Ru(NC)Ru(py)_4(CN)Ru(py)_4Cl](PF_6)_2$ (**2**) was prepared by reaction of *trans*-$Ru(CN)_2(py)_4$ with two equivalents of *trans*-$[RuCl(py)_4(Me_2CO)]^+$. Electronic coupling between the outer Ru(II) centers in **2** is significant, as evidenced by a $\Delta E_{1/2}$ value of *ca.* 100 mV for the $Ru^{III/II}$ couples. The chloride ligands in **2** are substituted in the presence of $AgCF_3CO_2$ in refluxing acetonitrile/water to give the symmetrical derivative *trans*-$[(MeCN)(py)_4Ru(NC)Ru(py)_4(CN)Ru(py)_4(MeCN)](PF_6)_4$ (**3**). This transformation causes a marked increase in the electronic coupling through the central Ru unit, as evidenced by a $\Delta E_{1/2}$ value of 280 mV for the outer $Ru^{III/II}$ couples in **3**. The single-crystal X-ray structures of *trans*-$Ru(CN)_2(py)_4\cdot 2CH_3CN$ and *trans*-$[Cl(py)_4Ru(NC)Ru(py)_4(CN)Ru(py)_4Cl](PF_6)_2\cdot 5CH_3CN\cdot C_5H_5N$ (**2**·$5CH_3CN$·C_5H_5N) have been determined. The complex *trans*-$Ru(CN)_2(py)_4\cdot 2CH_3CN$, chemical formula $C_{26}H_{26}N_8Ru$, crystallizes in the orthorhombic system, space group *Pbcn* with $a = 10.4714(11)$ Å, $b = 15.0098(18)$ Å, $c = 16.1018(15)$ Å, and $Z = 4$. The salt **2**·$5CH_3CN\cdot C_5H_5N$, chemical formula $C_{77}H_{80}Cl_2F_{12}N_{20}P_2Ru_3$, crystallizes in the orthorhombic system, space group *Pnnm* with $a = 14.882(7)$ Å, $b = 23.197(6)$ Å, $c = 24.034(7)$ Å, and $Z = 4$. The binding of two *trans*-$\{RuCl(py)_4\}^+$ groups has very little effect on the geometry of the *trans*-$Ru(CN)_2(py)_4$ unit. The complex in **2** has an almost perfectly linear geometry with eclipsed *trans*-$\{Ru(py)_4\}^{2+}$ units, and bond lengths indicating $d\pi(Ru^{II}) \rightarrow \pi^*(CN)$ back-bonding from both C- and N-bonded Ru centers. The Ru−Cl bond length is 2.4212(24) Å.

Introduction

The preparation and study of polynuclear, cyano-bridged metal complexes have attracted considerable interest over the past decade.[1−13] Intermetallic electronic coupling provided by the cyanide bridge has led to novel mixed-valence properties, and photoinduced electron- and energy-transfer have been observed. Of particular note is the demonstration that the trimetallic ruthenium complex *cis*-$[NC(bpy)_2Ru^{II}(CN)Ru^{II}(dcbpy)_2(NC)Ru^{II}(bpy)_2CN]^{2-}$ (bpy = 2,2′-bipyridine, dcbpy = 4,4′-dicarboxy-2,2′-bipyridine dianion) can serve as an efficient light-harvesting "antenna" in the sensitization of TiO_2-based photovoltaic cells.[14] Also of great significance is the recent report of *cis*-$\{Ru(bpy)_2\}^{2+}$-based oligomers which function as molecular conduits for long-range electronic energy transfer.[15]

With few exceptions,[6d,7] a common aspect of all existing polynuclear cyano-bridged complexes is that the bridging metal unit(s) have a *cis* geometry. This reduces the separation between bridged metal centers, and can also lead to structural and optical isomerism, for example in *cis*-$\{Ru(bpy)_2\}^{2+}$-based complexes. The utilization of *trans* bridging units would yield structurally well-defined assemblies in which long-range processes could be studied over extended distances. Such complexes containing a sufficiently large number of metal centers could be of interest as potential metal-based "molecular wires".[16]

We have been investigating routes for the controlled synthesis of *trans* complexes of Ru(II), and have used reactions of *trans*-$\{Ru(bpy)_2\}^{2+}$ complexes[17] to prepare a number of chromophore-

† Present address: Department of Chemistry, The University of Manchester, Oxford Road, Manchester M13 9PL, U.K.

⊗ Abstract published in *Advance ACS Abstracts,* June 1, 1995.

(1) Bignozzi, C. A.; Scandola, F. *Inorg. Chem.* **1984**, *23*, 1540.
(2) (a) Bignozzi, C. A.; Roffia, S.; Scandola, F. *J. Am. Chem. Soc.* **1985**, *107*, 1644. (b) Roffia, S.; Paradisi, C.; Bignozzi, C. A. *J. Electroanal. Chem.* **1986**, *200*, 105. (c) Bignozzi, C. A.; Paradisi, C.; Roffia, S.; Scandola, F. *Inorg. Chem.* **1988**, *27*, 408.
(3) Scandola, F.; Indelli, M. T.; Chiorboli, C.; Bignozzi, C. A. *Top. Curr. Chem.* **1990**, *158*, 73.
(4) Balzani, V.; Scandola, F. *Supramolecular Photochemistry*; Ellis Horwood: Chichester, U.K., 1991.
(5) (a) Bignozzi, C. A.; Roffia, S.; Chiorboli, C.; Davila, J.; Indelli, M. T.; Scandola, F. *Inorg. Chem.* **1989**, *28*, 4350. (b) Roffia, S.; Casadei, R.; Paolucci, F.; Paradisi, C.; Bignozzi, C. A.; Scandola, F. *J. Electroanal. Chem.* **1991**, *302*, 157.
(6) (a) Bignozzi, C. A.; Indelli, M. T.; Scandola, F. *J. Am. Chem. Soc.* **1989**, *111*, 5192. (b) Bignozzi, C. A.; Bortolini, O.; Chiorboli, C.; Indelli, M. T.; Rampi, M. A.; Scandola, F. *Inorg. Chem.* **1992**, *31*, 172. (c) Bignozzi, C. A.; Chiorboli, C.; Indelli, M. T.; Scandola, F.; Bertolasi, V.; Gilli, G. *J. Chem. Soc., Dalton Trans.* **1994**, 2391. (d) Indelli, M. T.; Scandola, F. *J. Phys. Chem.* **1993**, *97*, 3328.
(7) (a) Zhou, M.; Pfennig, B. W.; Steiger, J.; Van Engen, D.; Bocarsly, A. B. *Inorg. Chem.* **1990**, *29*, 2456. (b) Pfennig, B. W.; Bocarsly, A. B. *Coord. Chem. Rev.* **1991**, *111*, 91. (c) Pfennig, B. W.; Bocarsly, A. B. *J. Phys. Chem.* **1992**, *96*, 226.
(8) Bignozzi, C. A.; Argazzi, R.; Chiorboli, C.; Roffia, S.; Scandola, F. *Coord. Chem. Rev.* **1991**, *111*, 261.
(9) Kalyanasundaram, K.; Grätzel, M.; Nazeeruddin, M. K. *Inorg. Chem.* **1992**, *31*, 5243.
(10) Bignozzi, C. A.; Argazzi, R.; Schoonover, J. R.; Gordon, K. C.; Dyer, R. B.; Scandola, F. *Inorg. Chem.* **1992**, *31*, 5260.
(11) Teixeira, M. G.; Roffia, S.; Bignozzi, C. A.; Paradisi, C.; Paolucci, F. *J. Electroanal. Chem.* **1993**, *345*, 243.
(12) Scandola, F.; Argazzi, R.; Bignozzi, C. A.; Chiorboli, C.; Indelli, M. T.; Rampi, M. A. *Coord. Chem. Rev.* **1993**, *125*, 283.
(13) Bignozzi, C. A.; Argazzi, R.; Chiorboli, C.; Scandola, F.; Dyer, R. B.; Schoonover, J. R.; Meyer, T. J. *Inorg. Chem.* **1994**, *33*, 1652.
(14) (a) Amadelli, R.; Argazzi, R.; Bignozzi, C. A.; Scandola, F. *J. Am. Chem. Soc.* **1990**, *112*, 7099. (b) Nazeeruddin, M. K.; Liska, P.; Moser, J.; Vlachopoulos, N.; Grätzel, M. *Helv. Chim. Acta* **1990**, *73*, 1788. (c) O'Regan, B.; Grätzel, M. *Nature* **1991**, *353*, 737.
(15) Bignozzi, C. A.; Argazzi, R.; Garcia, C. G.; Scandola, F.; Schoonover, J. R.; Meyer, T. J. *J. Am. Chem. Soc.* **1992**, *114*, 8727.
(16) (a) Lehn, J.-M. *Angew. Chem., Int. Ed. Engl.* **1990**, *29*, 1304. (b) Vögtle, F. *Supramolecular Chemistry*; Wiley: Chichester, U.K., 1991; p 313. (c) Schumm, J. S.; Pearson, D. L.; Tour, J. M. *Angew. Chem. Int., Ed. Engl.* **1994**, *33*, 1360 and references therein.
(17) Coe, B. J.; Meyer, T. J.; White, P. S. *Inorg. Chem.* **1993**, *32*, 4012.

0020-1669/95/1334-3600$09.00/0

Table 1. UV−Visible and Electrochemical Data in Acetonitrile

complex	$E_{1/2}$ ($Ru^{III/II}$), V vs SCE (ΔE_p, mV)[a]	λ_{max}, nm (ϵ, M^{-1} cm^{-1})[b]	assignment
trans-$[Ru(OCH_3)_2(py)_4]PF_6$	−0.82 (70)[c]	198 (29 100)	$\pi \rightarrow \pi^*$
		242 (13 600)	$\pi \rightarrow \pi^*$
		316 (11 300)	$\pi \rightarrow d\pi$
		416 (5 400)	$\pi \rightarrow d\pi$
trans-$Ru(CN)_2(py)_4$[d]	0.80 (90)	204 (27 800)	$\pi \rightarrow \pi^*$
		248 (15 500)	$\pi \rightarrow \pi^*$
		374 (22 500)	$d\pi \rightarrow \pi^*$(py)
trans-$[Cl(py)_4Ru(NC)Ru(py)_4(CN)]PF_6$ (**1**)	1.20 (70)	200 (58 900)	$\pi \rightarrow \pi^*$
	0.53 (70)	218 sh (33 300)	$\pi \rightarrow \pi^*$
		248 (35 500)	$\pi \rightarrow \pi^*$
		372 (42 600)	$d\pi \rightarrow \pi^*$(py)
trans-$[Cl(py)_4Ru(NC)Ru(py)_4(CN)Ru(py)_4Cl](PF_6)_2$ (**2**)	1.51 (75)	208 (53 700)	$\pi \rightarrow \pi^*$
	0.64 (70)	226 (50 900)	$\pi \rightarrow \pi^*$
	0.54 (75)	248 (51 900)	$\pi \rightarrow \pi^*$
		306 sh (15 900)	$\pi \rightarrow \pi^*$
		370 (51 800)	$d\pi \rightarrow \pi^*$(py)
trans-$[(MeCN)(py)_4Ru(NC)Ru(py)_4(CN)Ru(py)_4(MeCN)](PF_6)_4$ (**3**)	1.65 (100)	196 (72 200)	$\pi \rightarrow \pi^*$
	1.31 (75)	234 (85 900)	$\pi \rightarrow \pi^*$
	1.03 (70)	276 (21 200)	$\pi \rightarrow \pi^*$
		346 (57 000)	$d\pi \rightarrow \pi^*$(py)

[a] Measured in solutions *ca.* 10^{-3} M in complex and 0.1 M in $[N(C_4H_9\text{-}n)_4]PF_6$ at a Pt disk working electrode (surface area 0.031 cm^2) with a scan rate of 200 mV s^{-1}. Ferrocene internal reference $E_{1/2}$ = 0.42 V, ΔE_p = 70 mV. [b] Solutions *ca.* 5 × 10^{-5} M. [c] Also shows an irreversible oxidation at E_{pa} = 0.74 V. [d] From reference 19.

quencher derivatives.[18] The dicyano complex *trans*-$Ru(CN)_2(bpy)_2$ is known,[17] but its total insolubility in all common solvents precludes its use as a precursor for the synthesis of cyano-bridged assemblies. Other work with *trans*-$\{Ru(py)_4\}^{2+}$ complexes has yielded the readily soluble *trans*-$Ru(CN)_2(py)_4$[19] which is a promising starting point for further syntheses. The highly stable *trans*-$\{Ru(py)_4\}^{2+}$ center appears ideal for this purpose, acting as a visible nonchromophoric spacer due to the typically high energy of the $Ru^{II} \rightarrow$ py MLCT absorptions.

Experimental Section

Materials and Procedures. The complex *trans*-$Ru(CN)_2(py)_4 \cdot H_2O$ and the salt *trans*-$[RuCl(py)_4(NO)](PF_6)_2$ were prepared according to previously published procedures.[19] All other reagents were obtained commercially and used as supplied. All reactions were conducted under an atmosphere of argon. Products were dried at room temperature in a vacuum desiccator for *ca.* 15 h prior to characterization.

Physical Measurements. ^1H NMR spectra were recorded on a Bruker AC200 spectrometer and all shifts are referenced to TMS. The signals for pyridine protons show fine splitting at this field, but are reported here as simple multiplets. Elemental analyses were performed by ORS, Whitesboro, NY. IR spectra were obtained as KBr disks with a Mattson Galaxy Series FTIR 5000 instrument. UV−visible spectra were recorded by using a Hewlett-Packard 8451A diode array spectrophotometer. FAB mass spectra were recorded by ORS, Whitesboro, NY, by using an 8 keV Ar atom beam and 3-nitrobenzyl alcohol as matrix. The magnetic moment of *trans*-$[Ru(OCH_3)_2(py)_4]PF_6$ was measured by the Gouy method on a Johnson Matthey magnetic susceptibility balance with $Hg[Co(SCN)_4]$ as the calibration standard.

Cyclic voltammetric measurements were carried out by using a PAR Model 173 potentiostat with a PAR Model 175 universal programmer. A three-compartment cell was used with an SCE reference electrode separated from a Pt disk working electrode (surface area 0.031 cm^2) and Pt wire auxiliary electrode by a medium porosity glass frit. Spectrophotometric grade acetonitrile (Burdick and Jackson) was used as received and tetra-*n*-butylammonium hexafluorophosphate, $[N(n\text{-}C_4H_9)_4]PF_6$, doubly recrystallized from ethanol and dried in vacuo, was used as supporting electrolyte. Solutions containing 10^{-3} M analyte (0.1 M electrolyte) were deaerated for 5 min by a vigorous Ar purge. All $E_{1/2}$ values were calculated from $(E_{pa} + E_{pc})/2$ at a scan rate of 200 mV s^{-1} with no correction for junction potentials.

Reaction of *trans*-$[RuCl(py)_4(Me_2CO)]^+$ with Cyanide Ion. A solution of *trans*-$[RuCl(py)_4(NO)](PF_6)_2$ (400 mg, 0.518 mmol) and NaN_3 (35.5 mg, 0.546 mmol) in acetone (12 mL) was stirred at room temperature for 1.5 h. A solution of $[Et_4N]CN$ (87 mg, 0.557 mmol) in methanol (6 mL) was added, causing an immediate color change from dark golden to red. The solution was stirred at room temperature for 20 h, during which time an orange precipitate formed. The mixture was concentrated to *ca.* 2 mL on a rotary evaporator, and the solid was collected by filtration, washed with methanol and then water, and dried (158 mg). The dark golden filtrate solution was not investigated further. The solid was dissolved in dichloromethane and loaded onto a silica column (dimensions 30 × 2.5 cm). Three bands were collected using a solvent gradient from 100% dichloromethane to 100% acetone. The first band, eluted with 5% acetone/dichloromethane was evaporated to yield a golden-orange solid. This was identified by TLC and ^1H NMR and IR spectra as *trans*-$RuCl_2(py)_4$ (yield 74 mg, 29%). Elution with 10% acetone/dichloromethane gave a second band which was evaporated to yield a golden-orange solid (3 mg). This contained *ca.* 50% *trans*-$RuCl_2(py)_4$ together with 50% of another complex, assigned tentatively as *trans*-$RuCl(CN)(py)_4$ by ^1H NMR and IR spectra: δ_H (CD_2Cl_2) 8.41 (8 H, d, $H^{2,6}$ × 4), 7.67 (4 H, t, H^4 × 4), 7.14 (8 H, t, $H^{3,5}$ × 4); ν(CN) 2027 (s) cm^{-1}. The third and final band from the column, eluted with acetone, was evaporated to yield a golden solid (57 mg). This was recrystallized from acetonitrile/diethyl ether and identified as *trans*-$[Ru(OCH_3)_2(py)_4]PF_6$ (yield 51 mg, 16%); ν(C−H) 2908 (m), 2877 (m), 2796 (s) cm^{-1}; ν(C−O) 1041 (s) cm^{-1}; $\nu(PF_6^-)$ 837 (vs) cm^{-1}; ν(Ru−O) 557 (s) cm^{-1}. Anal. Calcd for $C_{22}H_{26}F_6N_4O_2$-PRu: C, 42.31; H, 4.20; N, 8.97. Found: C, 42.17; H, 4.14; N, 9.10. (Note: An identical reaction run for 90 h yielded 44 mg of *trans*-$RuCl_2(py)_4$ and 88 mg of *trans*-$[Ru(OCH_3)_2(py)_4]PF_6$.)

Synthesis of *trans*-$[Cl(py)_4Ru(NC)Ru(py)_4(CN)]PF_6$ (1). A solution of *trans*-$[RuCl(py)_4(NO)](PF_6)_2$ (100 mg, 0.129 mmol) and NaN_3 (8.9 mg, 0.129 mmol) in acetone (3 mL) was stirred at room temperature for 1 h. Half of the resulting solvento complex solution was added dropwise to a stirred solution of *trans*-$Ru(CN)_2(py)_4 \cdot H_2O$ (643 mg, 1.32 mmol) in methanol (4 mL), and the reaction was stirred for 30 min. The remainder of the solvento complex was added and the solution stirred for a further 30 min. The solvents were evaporated, the solid dissolved in $CHCl_3$ (*ca.* 20 mL) and loaded onto a column of alumina (dimensions 30 × 2.5 cm). The initial golden fraction eluted in $CHCl_3$ was discarded, and the major yellow fraction evaported to yield unreacted *trans*-$Ru(CN)_2(py)_4 \cdot H_2O$. Using a solvent gradient of 1−4% methanol/$CHCl_3$, a golden band was collected and evaporated to yield

(18) Coe, B. J.; Friesen, D. A.; Thompson, D. W.; Meyer, T. J. Manuscript in preparation.
(19) Coe, B. J.; Meyer, T. J.; White, P. S. *Inorg. Chem.* **1995**, *34*, 593.

the crude product (109 mg). Further purification was achieved by slow recrystallization from CH_3CN/pyridine/diethyl ether. The product was precipitated from CH_3CN/diethyl ether to eliminate solvent(s) of crystallization, collected by filtration, washed with diethyl ether and dried to afford a golden solid: yield 96 mg, 70%; δ_H (CD_3COCD_3) 8.48−8.40 (16 H, c m, $H^{2,6} \times 8$), 7.93−7.82 (8 H, c m, $H^4 \times 8$), 7.20−7.12 (16 H, c m, $H^{3,5} \times 8$); ν(CN) 2064 (s) cm^{-1}. Anal. Calcd for $C_{42}H_{40}ClF_6N_{10}PRu_2 \cdot H_2O$: C, 46.48; H, 3.90; N, 12.90. Found: C, 46.17; H, 3.77; N, 12.89.

Synthesis of *trans*-[Cl(py)$_4$Ru(NC)Ru(py)$_4$(CN)Ru(py)$_4$Cl](PF$_6$)$_2$ (2). A solution of *trans*-[RuCl(py)$_4$(NO)](PF$_6$)$_2$ (200 mg, 0.259 mmol) and NaN_3 (17.8 mg, 0.274 mmol) in acetone (6 mL) was stirred at room temperature for 1 h. Acetone (3 mL) and *trans*-Ru(CN)$_2$(py)$_4$·H_2O (62 mg, 0.127 mmol) were added, and the solution was stirred in the dark for a further 3 d. The addition of water (50 mL) afforded a mustard yellow precipitate which was collected by filtration, washed with water, and dried. Purification was effected by passage through a short column of alumina (dimensions 15 × 1.5 cm) in acetone followed by recrystallization from CH_3CN/pyridine/diethyl ether. The product was precipitated from CH_3CN/diethyl ether to eliminate solvent(s) of crystallization, collected by filtration, washed with diethyl ether and dried to afford a golden solid: yield 122 mg, 57%; δ_H (CD_3COCD_3) 8.37 (16 H, d, $H^{2,6}_{outer} \times 8$), 8.28 (8 H, d, $H^{2,6}_{central} \times 4$), 7.95 (4 H, t, $H^4_{central} \times 4$), 7.85 (8 H, t, $H^4_{outer} \times 8$), 7.18−7.08 (24 H, c m, $H^{3,5} \times 12$); ν(CN) 2067 (m) cm^{-1}. Anal. Calcd for $C_{62}H_{60}Cl_2F_{12}N_{14}P_2Ru_3$: C, 44.72; H, 3.63; N, 11.78. Found: C, 44.42; H, 3.82; N, 11.77. (Note: A slightly reduced yield of 117 mg (54%) was obtained using the same procedure, except with a reaction time of 2 h at reflux after the addition of *trans*-Ru(CN)$_2$(py)$_4$·H_2O.)

Synthesis of *trans*-[(MeCN)(py)$_4$Ru(NC)Ru(py)$_4$(CN)Ru(py)$_4$(MeCN)](PF$_6$)$_4$ (3). A solution of **2** (40 mg, 0.024 mmol) and $AgCF_3CO_2$ (25 mg, 0.113 mmol) in acetonitrile (6 mL) and water (3 mL) was stirred at reflux in the dark for 9 h. The addition of aqueous NH_4PF_6 afforded a cream precipitate which was collected by filtration, washed with water and dried. The product was dissolved through the frit in acetonitrile to leave AgCl, and purified by passage through a short column of alumina (dimensions 5 × 0.5 cm) in acetonitrile followed by recrystallization from CH_3CN/diethyl ether. The product was precipitated from CH_3CN/diethyl ether to eliminate solvent(s) of crystallization, collected by filtration, washed with diethyl ether and dried to afford a cream solid: yield 43 mg, 91%; δ_H (CD_3COCD_3) 8.31 (24 H, d, $H^{2,6} \times 12$), 8.03−7.90 (12 H, c m, $H^4 \times 12$), 7.30 (16 H, t, $H^{3,5}_{outer} \times 8$), 7.16 (8 H, t, $H^{3,5}_{central} \times 4$), 2.73 (6 H, s, MeCN × 2); ν(CN) 2077 (m) cm^{-1}. Anal. Calcd for $C_{66}H_{66}F_{24}N_{16}P_4Ru_3 \cdot H_2O$: C, 39.95; H, 3.45; N, 11.29. Found: C, 39.76; H, 3.22; N, 11.34.

X-ray Structural Determinations. Suitable crystals of *trans*-Ru(CN)$_2$(py)$_4$ and *trans*-[Cl(py)$_4$Ru(NC)Ru(py)$_4$(CN)Ru(py)$_4$Cl](PF$_6$)$_2$ (**2**) were grown by slow diffusion of diethyl ether vapor into acetonitrile/pyridine solutions at room temperature. A pale yellow crystal of *trans*-Ru(CN)$_2$(py)$_4$ of dimensions 0.35 × 0.35 × 0.20 mm, and a golden crystal of **2** of dimensions 0.45 × 0.25 × 0.25 mm were selected for diffraction study. Data were collected on a Rigaku AFC6/S diffractometer by using the ω scan mode with graphite-monochromated Mo Kα radiation (λ = 0.710 73 Å). Crystallographic data and refinement details are presented in Table 2. Accurate cell constants were obtained from least-squares fits using a total of 122 and 48 high-angle reflections, $30.00 \le 2\theta \le 40.00°$, for *trans*-Ru(CN)$_2(py)_4$ and for **2**, respectively. For *trans*-Ru(CN)$_2$(py)$_4$, of the 2226 unique reflections measured, 1546 reflections with $I > 2.5\sigma(I)$ were used in the structure solution and subsequent refinement. For **2**, 2910 of 5595 unique reflections had $I > 2.5\sigma(I)$. Final agreement indices obtained with hydrogen atoms placed in their calculated positions are: for *trans*-Ru(CN)$_2$(py)$_4$, R = 2.6% and R_w = 3.5%; for **2**, R = 4.8% and R_w = 5.7%. Weights were estimated from counting statistics.

The crystal of *trans*-Ru(CN)$_2$(py)$_4$ contains 2.0 molecules of acetonitrile per asymmetric unit. The crystal of **2** contains 5.0 molecules of acetonitrile and 1.0 molecules of pyridine per asymmetric unit. Of these, two volumes of solvent are disordered; these were modeled with seven carbon atoms placed in fixed positions and only their isotropic thermal parameters were permitted to refine. These appear to be a disordered acetonitrile (S1−S3) and a pyridine (S4−S7). The correct empirical formula is $C_{62}H_{60}Cl_2F_{12}N_{14}P_2Ru_3 \cdot 5(C_2H_3N) \cdot C_5H_5N$. The formula given in Table 2 is based on the actual contents of the model unit cell. No correction was made for absorption. ORTEP[20] diagrams showing views of the complex *trans*-Ru(CN)$_2$(py)$_4$ and of the cation in **2** are given in Figures 4, 5, and 6. Crystallographic data and refinement details are given in Table 2, selected bond distances in Tables 3 and 4, selected bond angles in Tables 5 and 6, and final atomic fractional coordinates in Tables 7 and 8. Anisotropic thermal parameters, hydrogen atomic parameters, and all nonessential bond lengths and angles are provided as supplementary material. All computations

Table 2. Crystallographic Data and Refinement Details for *trans*-Ru(CN)$_2$(py)$_4$·2MeCN and [Cl(py)$_4$Ru(NC)Ru(py)$_4$(CN)Ru(py)$_4$Cl](PF$_6$)$_2$·5MeCN·py (**2**·5MeCN·py)

	trans-Ru(CN)$_2$(py)$_4$·2MeCN	**2**·5MeCN·py
formula	$C_{26}H_{26}N_8Ru$	$C_{79}H_{72}Cl_2F_{12}N_{18}P_2Ru_3$
fw	553.63	1937.58
space group	*Pbcn*, orthorhombic	*Pnnm*, orthorhombic
a, Å	10.4714(11)	14.882(7)
b, Å	15.0098(18)	23.197(6)
c, Å	16.1018(15)	24.034(7)
V, Å^3	2530.8(5)	8297(5)
Z	4	4
D_{calc}, Mg m^{-3}	1.453	1.551
T, K	138	128
λ (Mo Kα), Å	0.710 73	0.710 73
F(000)	1130.69	3890.44
μ, mm^{-1}	0.64	0.68
scan type	ω	ω
2θ limit, deg	50	45
h, k, l ranges	0−12, 0−17, 0−19	0−16, 0−25, 0−25
tot. no. of reflcns	2227	6882
no. of unique reflcns	2226	5595
no. of data with $I > 2.5\sigma(I)$	1546	2910
R^a	0.026	0.048
$R_w{}^a$	0.035	0.057
GOF	1.18	1.60
no. of params	162	515
max res elec dens, e/Å^3	0.30	0.99
min res elec dens, e/Å^3	−0.69	−0.65

^{a} $R = \sum(|F_o| - |F_c|)/\sum|F_o|$; $R_w = [\sum w(F_o - F_c)^2/\sum wF_o^2]^{1/2}$; GOF = $[\sum w(F_o - F_c)^2/(\text{no. of reflcns} - \text{no. of params})]^{1/2}$.

Table 3. Selected Bond Distances (Å) for *trans*-Ru(CN)$_2$(py)$_4$·2MeCN

Ru(1)−C(1)	2.057(4)	Ru(1)−N(21)	2.093(4)
Ru(1)−C(1)a	2.057(4)	Ru(1)−N(31)	2.090(4)
Ru(1)−N(11)	2.091(3)	C(1)−N(1)	1.156(5)
Ru(1)−N(11)a	2.091(3)		

Table 4. Selected Bond Distances (Å) for **2**·5MeCN·py

Ru(1)−C(1)	2.040(10)	Ru(2)−N(1)	2.013(8)
Ru(1)−C(1)a	2.040(10)	Ru(2)−N(31)	2.090(9)
Ru(1)−N(11)	2.096(8)	Ru(2)−N(41)	2.068(9)
Ru(1)−N(11)a	2.096(8)	Ru(2)−N(61)	2.074(9)
Ru(1)−N(21)	2.090(9)	Ru(2)−N(51)	2.078(8)
Ru(1)−N(21)a	2.090(9)	C(1)−N(1)	1.157(12)
Ru(2)−Cl(1)	2.4212(24)		

Table 5. Selected Bond Angles (deg) for *trans*-Ru(CN)$_2$(py)$_4$·2MeCN

C(1)−Ru(1)−C(1)a	179.92(21)	Cl(1)a−Ru(1)−N(31)	89.93(9)
C(1)−Ru(1)−N(11)	89.86(11)	N(11)−Ru(1)−N(11)a	179.87(13)
C(1)−Ru(1)−N(11)a	90.14(11)	N(11)−Ru(1)−N(21)	89.91(7)
C(1)−Ru(1)−N(21)	90.07(9)	N(11)−Ru(1)−N(31)	90.09(7)
C(1)−Ru(1)−N(31)	89.93(9)	N(11)a−Ru(1)−N(21)	89.91(7)
C(1)a−Ru(1)−N(11)	90.14(11)	N(11)a−Ru(1)−N(31)	90.09(7)
C(1)a−Ru(1)−N(11)a	89.86(11)	N(21)−Ru(1)−N(31)	179.9
C(1)a−Ru(1)−N(21)	90.07(9)	Ru(1)−C(1)−N(1)	179.4(3)

(20) Johnson, C. K. *ORTEP: A fortran thermal ellipsoid plot program*; Technical Report ORNL-5138; Oak Ridge National Laboratory: Oak Ridge, TN, 1976.

Table 6. Selected Bond Angles (deg) for **2**·5MeCN·py

C(1)−Ru(1)−C(1)a	177.6(5)	Cl(1)−Ru(2)−N(31)	89.5(3)
C(1)−Ru(1)−N(11)	89.3(4)	Cl(1)−Ru(2)−N(41)	89.2(3)
C(1)−Ru(1)−N(11)a	92.5(4)	Cl(1)−Ru(2)−N(61)	91.4(3)
C(1)−Ru(1)−N(21)	89.3(4)	Cl(1)−Ru(2)−N(51)	91.1(3)
C(1)−Ru(1)−N(21)a	89.1(4)	N(1)−Ru(2)−N(31)	88.2(3)
C(1)a−Ru(1)−N(11)	92.5(4)	N(1)−Ru(2)−N(41)	90.1(4)
C(1)a−Ru(1)−N(11)a	89.3(4)	N(1)−Ru(2)−N(61)	90.9(3)
C(1)a−Ru(1)−N(21)	89.1(4)	N(1)−Ru(2)−N(51)	89.7(3)
C(1)a−Ru(1)−N(21)a	89.3(4)	N(31)−Ru(2)−N(41)	92.7(3)
N(11)−Ru(1)−N(11)a	88.8(4)	N(31)−Ru(2)−N(61)	178.1(3)
N(11)−Ru(1)−N(21)	88.8(3)	N(31)−Ru(2)−N(51)	88.6(3)
N(11)−Ru(1)−N(21)a	177.0(4)	N(41)−Ru(2)−N(61)	88.9(3)
N(11)a−Ru(1)−N(21)	177.0(4)	N(41)−Ru(2)−N(51)	178.6(4)
N(11)a−Ru(1)−N(21)a	88.8(3)	N(61)−Ru(2)−N(51)	89.7(3)
N(21)−Ru(1)−N(21)a	93.7(4)	Ru(1)−C(1)−N(1)	177.8(9)
Cl(1)−Ru(2)−N(1)	177.59(21)	Ru(2)−N(1)−C(1)	176.6(9)

Table 7. Final Atomic Fractional Coordinates and Equivalent Isotropic Displacement Coefficients (Å²) for *trans*-Ru(CN)₂(py)₄·2MeCN

atom	*x*	*y*	*z*	B_{iso}[a]
Ru(1)	0	0.185215(21)	1/4	1.050(16)
C(1)	−0.1924(3)	0.18506(21)	0.22419(20)	1.38(13)
N(1)	−0.3007(3)	0.18449(18)	0.21031(20)	2.02(12)
N(11)	0.03984(25)	0.18542(16)	0.12276(17)	1.24(10)
C(12)	0.1279(3)	0.24102(22)	0.08988(20)	1.67(13)
C(13)	0.1570(3)	0.24313(23)	0.00672(22)	1.89(13)
C(14)	0.0961(4)	0.18548(23)	−0.04691(21)	2.12(15)
C(15)	0.0053(4)	0.12789(22)	−0.01421(21)	2.05(14)
C(16)	−0.0211(3)	0.13007(22)	0.06940(21)	1.63(12)
N(21)	0	0.32469(23)	1/4	1.45(15)
C(22)	−0.0759(3)	0.37198(22)	0.19846(21)	1.63(13)
C(23)	−0.0792(3)	0.46361(23)	0.19699(22)	2.02(14)
C(24)	0	0.5107(3)	1/4	2.23(21)
N(31)	0	0.04600(23)	1/4	1.22(14)
C(32)	0.1011(3)	−0.00143(23)	0.22218(21)	1.56(13)
C(33)	0.1039(3)	−0.09330(23)	0.22178(22)	1.89(13)
C(34)	0	−0.1407(3)	1/4	1.96(20)
C(41)	0.4209(4)	1.1209(3)	0.0698(3)	3.60(19)
C(42)	0.3508(4)	1.0390(3)	0.0504(3)	3.09(18)
N(43)	0.2958(4)	0.9762(3)	0.0360(3)	4.74(20)

[a] B_{iso} is the mean of the principal axes of the thermal ellipsoid.

were performed by using the NRCVAX[21] suite of programs. Atomic scattering factors were taken from a standard source[22] and corrected for anomalous dispersion.

Results and Discussion

Synthetic Studies. A number of complexes of the form *trans*-$[RuCl(py)_4(L)]^+$ (L = N-heterocycle) have been prepared by reaction of the acetone solvento complex, *trans*-$[RuCl(py)_4(Me_2CO)]^+$, with ligands L.[19] The solvento intermediate is prepared by azide-assisted labilization of the nitrosyl ligand in *trans*-$[RuCl(py)_4(NO)]^{2+}$. Reaction of *trans*-$[RuCl(py)_4(Me_2CO)]^+$ with cyanide ion should yield *trans*-$RuCl(CN)(py)_4$. This complex could perhaps be used to synthesize linear oligomeric assemblies of formula *trans*-$[ClRu^{II}(py)_4\{(CN)Ru^{II}(py)_4(CN)\}_n Ru^{II}(py)_4(CN)]^{(n+1)+}$ (n = 1,2, *etc.*).[23] If end-capped with redox-active or photoactive metal centers, these would provide a useful comparison to the recently reported *cis*-$\{Ru(bpy)_2\}^{2+}$-based oligomers in which long-range electronic energy transfer was observed.[15]

(21) Gabe, E. J.; Le Page, Y.; Charland, J.-P.; Lee, F. L.; White, P. S. *J. Appl. Crystallogr.* **1989**, *22*, 384.
(22) *International Tables for X-ray Crystallography*; Kynoch Press: Birmingham, U.K., 1974; Vol. IV.
(23) Although an oligomerization reaction of *trans*-$RuCl(CN)(py)_4$ would be inherently uncontrollable, it might be possible to adopt a strategy similar to that described in ref 15 whereby a mixture of oligomers is formed, end-capped with a suitable metal center, and then separated chromatographically.

Table 8. Final Atomic Fractional Coordinates and Equivalent Isotropic Displacement Coefficients (Å²) for **2**·5MeCN·py

atom	*x*	*y*	*z*	B_{iso}[a]
Ru(1)	0	0	0.25553(5)	1.17(4)
Ru(2)	0.24609(5)	0.15964(3)	0.25157(4)	1.25(3)
Cl(1)	0.36590(16)	0.23023(9)	0.25334(13)	2.03(11)
C(1)	0.0968(6)	0.0622(4)	0.2537(5)	1.5(4)
N(1)	0.1501(5)	0.0985(3)	0.2514(4)	1.3(4)
P(1)	0.6280(3)	0.09698(19)	0	1.43(20)
P(2)	0.6167(4)	0.09860(21)	1/2	2.14(24)
N(11)	−0.0669(6)	0.0464(4)	0.3178(4)	1.5(4)
C(12)	−0.1570(7)	0.0492(5)	0.3192(5)	2.6(6)
C(13)	−0.2051(8)	0.0790(5)	0.3591(5)	3.0(6)
C(14)	−0.1576(11)	0.1061(5)	0.4008(6)	3.7(7)
C(15)	−0.0648(9)	0.1043(5)	0.3988(5)	3.3(6)
C(16)	−0.0225(8)	0.0735(5)	0.3585(4)	2.5(5)
N(21)	−0.0727(7)	0.0463(4)	0.1961(4)	1.8(5)
C(22)	−0.0832(7)	0.1051(4)	0.2015(4)	1.9(5)
C(23)	−0.1329(8)	0.1359(4)	0.1634(5)	2.8(6)
C(24)	−0.1750(9)	0.1102(5)	0.1211(5)	3.2(7)
C(25)	−0.1632(9)	0.0515(5)	0.1150(5)	3.2(6)
C(26)	−0.1122(8)	0.0215(4)	0.1525(5)	2.1(5)
N(31)	0.3150(6)	0.1111(4)	0.3111(3)	1.3(4)
C(32)	0.4039(7)	0.1032(4)	0.3106(4)	1.7(5)
C(33)	0.4476(7)	0.0703(5)	0.3489(5)	2.5(5)
C(34)	0.4002(9)	0.0446(5)	0.3910(5)	2.7(6)
C(35)	0.3106(8)	0.0530(4)	0.3936(5)	2.2(6)
C(36)	0.2705(6)	0.0847(4)	0.3528(4)	1.4(5)
N(41)	0.3099(7)	0.1187(4)	0.1862(3)	1.6(4)
C(42)	0.3228(8)	0.0610(4)	0.1839(4)	1.9(5)
C(43)	0.3643(8)	0.0345(5)	0.1401(5)	2.9(6)
C(44)	0.3980(8)	0.0663(5)	0.0957(5)	2.4(6)
C(45)	0.3872(8)	0.1245(5)	0.0972(4)	2.7(6)
C(46)	0.3442(8)	0.1488(4)	0.1423(4)	2.2(5)
N(61)	0.1742(6)	0.2081(4)	0.1943(3)	1.5(4)
C(62)	0.1243(8)	0.1839(4)	0.1543(4)	2.1(5)
C(63)	0.0728(8)	0.2146(5)	0.1182(5)	2.7(6)
C(64)	0.0715(9)	0.2737(5)	0.1211(5)	2.7(6)
C(65)	0.1225(8)	0.2994(4)	0.1608(5)	2.4(5)
C(66)	0.1723(8)	0.2675(4)	0.1965(4)	1.9(5)
N(51)	0.1798(6)	0.2017(3)	0.3160(3)	1.4(4)
C(52)	0.2240(8)	0.2228(4)	0.3604(4)	2.0(5)
C(53)	0.1808(9)	0.2479(4)	0.4056(5)	2.4(6)
C(54)	0.0885(9)	0.2514(5)	0.4054(5)	2.6(6)
C(55)	0.0415(8)	0.2311(5)	0.3606(5)	2.3(5)
C(56)	0.0893(8)	0.2066(4)	0.3169(5)	2.0(5)
F(11)	0.6273(5)	0.0969(3)	0.06673(22)	2.4(3)
F(12)	0.7147(6)	0.0577(4)	0	2.6(4)
F(13)	0.6910(7)	0.1528(4)	0	3.1(5)
F(14)	0.5402(6)	0.1373(4)	0	2.6(4)
F(15)	0.5648(6)	0.0418(4)	0	2.7(4)
F(21)	0.6185(5)	0.0984(3)	0.43361(25)	3.1(3)
F(22)	0.6818(7)	0.0440(4)	1/2	3.7(5)
F(23)	0.7034(8)	0.1393(4)	1/2	3.8(5)
F(24)	0.5536(7)	0.1533(4)	1/2	3.6(5)
F(25)	0.5327(7)	0.0571(4)	1/2	3.7(5)
C(71)	0.2383(18)	0.2292(9)	0	7.7(17)
C(72)	0.3284(19)	0.2512(9)	0	4.5(12)
N(73)	0.3994(15)	0.2671(9)	0	6.5(12)
C(81)	0.5836(8)	0.1366(5)	0.1928(5)	3.2(6)
C(82)	0.6167(9)	0.0926(5)	0.2306(5)	3.2(6)
N(83)	0.6421(7)	0.0580(4)	0.2599(5)	4.3(6)
C(91)	0.8479(20)	0.3365(12)	0	9.2(18)
C(92)	0.8827(20)	0.2714(13)	0	7.0(17)
N(93)	0.9061(17)	0.2185(11)	0	8.8(16)
S(1)	0.64865	0.38438	0	9.7(8)
S(2)	0.60675	0.44777	0	18.1(16)
S(3)	0.54036	0.48393	0	18.0(16)
S(4)	0.12550	0.07966	0.04813	16.0(10)
S(5)	0.19323	0.07735	0	13.4(11)
S(6)	0.01412	0.08541	0	11.0(9)
S(7)	0.04932	0.08478	0.04516	35.3(25)

[a] B_{iso} is the mean of the principal axes of the thermal ellipsoid.

The solvento complex, *trans*-$[RuCl(py)_4(Me_2CO)]^+$, undergoes a rapid reaction with cyanide, as evidenced by an

Scheme 1. Suggested Reaction Sequence for *trans*-$[RuCl(py)_4(Me_2CO)]^+$ with Cyanide Ion

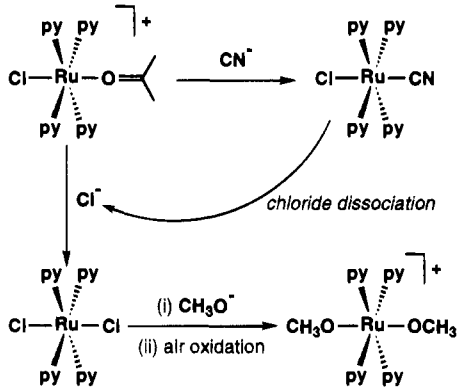

instantaneous color change. This is presumably due to formation of the desired *trans*-$RuCl(CN)(py)_4$, but we have been repeatedly unsuccessful in isolating this complex. Even after short reaction times of *ca.* 15 min, the major isolable product from these reactions is *trans*-$RuCl_2(py)_4$. The only reasonable mechanism for formation of this complex is via reaction of the solvento intermediate with chloride ion. The latter may be generated by chloride loss from *trans*-$RuCl(CN)(py)_4$ due to the strong *trans* labilizing effect of the CN^- ligand. When the reaction is allowed to proceed for a period of hours, the yield of *trans*-$RuCl_2(py)_4$ decreases. This is accompanied by an increasing yield of another product, identified as *trans*-$[Ru^{III}(OCH_3)_2(py)_4]^+$, probably resulting from reaction of *trans*-$RuCl_2(py)_4$ with methoxide ion. Although *trans*-$RuCl_2(py)_4$ precipitates when present in sufficient quantity, it is sparingly soluble in acetone/methanol and can hence continue to react. None of the complexes *trans*-$Ru(CN)_2(py)_4$, *trans*-$[RuCl(OCH_3)(py)_4]^+$, or *trans*-$Ru(CN)(OCH_3)(py)_4$ were isolated from these reactions. It is very likely that all three are produced, but do not precipitate upon concentration of the reaction solution. A proposed reaction sequence to explain this behavior is given in Scheme 1.

The effective magnetic moment of *trans*-$[Ru(OCH_3)_2(py)_4]PF_6$ is 1.95 μ_B at 22 °C.[24] This is close to the spin-only value for one unpaired electron, and similar values were reported for the related Ru(III) complexes *trans*-$[RuCl(OCH_3)(py)_4]^+$ and *trans*-$[RuCl(OH)(py)_4]^+$.[25] An attempted synthesis of *trans*-$RuCl(CN)(py)_4$ by reaction of *trans*-$Ru(CN)_2(py)_4$ with chloride was unsuccessful due to the inertness of the dicyano complex.[26]

The complex *trans*-$Ru(CN)_2(py)_4$[19] is an alternate starting point for the preparation of cyano-bridged *trans* assemblies. The asymmetrical bimetallic salt *trans*-$[Cl(py)_4Ru(NC)Ru(py)_4(CN)]PF_6$ (**1**) is readily prepared in high yield by reaction of *trans*-$[RuCl(py)_4(Me_2CO)]^+$ with a 10-fold excess of *trans*-$Ru(CN)_2(py)_4$. The symmetrical trimetallic salt *trans*-$[Cl(py)_4Ru(NC)Ru(py)_4(CN)Ru(py)_4Cl](PF_6)_2$ (**2**) can be prepared by reaction of **1** with further *trans*-$Ru(CN)_2(py)_4$, but is more conveniently synthesized in one step by reaction of *trans*-$Ru(CN)_2(py)_4$ with 2 equiv of *trans*-$[RuCl(py)_4(Me_2CO)]^+$. This reaction is slow at room temperature, but the yield is reduced only slightly by heating at reflux for a shorter time.

Scheme 2. Synthesis of Complexes **1**–**3**

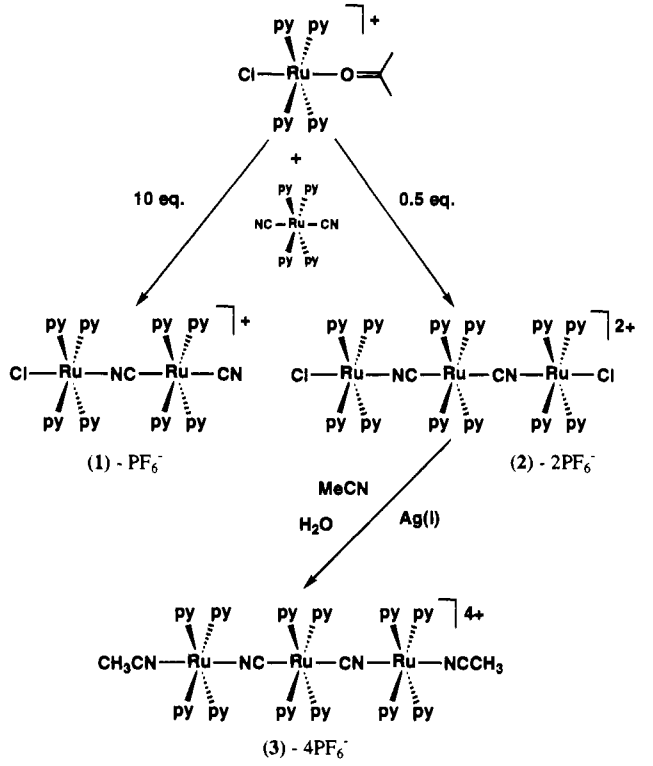

Thermally induced linkage isomerism of bridging cyanide ligands has been recently observed in the trinuclear complex *cis*-$[Ru^{II}(bpy)_2\{trans\text{-}Cr^{III}(cyclam)(CN)_2\}_2]^{4+}$.[6c] The arrangement of the cyanides in **1** and **2** (both C-bonded to one Ru) is dictated by the synthetic procedures used, assuming that no linkage isomerization occurs under the chosen reaction conditions. This is a reasonable assumption, given that such an isomerization requires high temperatures (*ca.* 150 °C),[6c] and the preparations of **1** and **2** involve only mild conditions. These structures are further supported by both infrared and electrochemical studies (*vide infra*).

The trimetallic complex *trans*-$[Cl(py)_4Ru^{II}(NC)Ru^{II}(py)_4(CN)Ru^{II}(py)_4Cl]^{2+}$ in **2** is of interest because it contains terminal chlorides which may be selectively substituted, thus opening the way to the construction of extended linear systems. Despite a comparatively long Ru–Cl bond length of 2.4212(24) Å (*vide infra*), the chloride ligands in **2** are substituted very slowly by $AgCF_3CO_2$ in refluxing acetonitrile. This reaction is faster in the presence of water, giving a symmetrical derivative *trans*-$[(MeCN)(py)_4Ru(NC)Ru(py)_4(CN)Ru(py)_4(MeCN)](PF_6)_4$ (**3**). It is assumed that no linkage isomerization occurs in this reaction. In the complex *cis*-$[Ru^{II}(bpy)_2\{trans\text{-}Cr^{III}(cyclam)(CN)_2\}_2]^{4+}$,[6c] isomerization was not observed after heating at 60 °C for 60 h in aqueous solution, but only upon heating for several hours at 150 °C in a KBr disk. Prolonged heating of the reaction to form **3** (beyond 9 h) gives no change in either the yield or identity of the product. Furthermore, *trans*-$Ru(CN)_2(py)_4$ is remarkably inert to substitution reactions,[26]

(24) This was calculated by using a mixture of published and estimated diamagnetic susceptibility values (all are -1×10^{-6}/g ion or molecule). For py and Ru^{3+} the reported values (49 and 23, respectively) were used. The values for PF_6^- and OCH_3^- were approximated as being the same as those for BF_4^- (39) and OH^- (12), respectively. Sources: py from Mabbs, F. E.; Machin, D. J. *Magnetism and Transition Metal Complexes*; Chapman and Hall: London, U.K., 1973; Ru^{3+}, BF_4^-, and OH^- from Mulay, L. N.; Boudreaux, E. A. *Theory and Applications of Molecular Diamagnetism*; Wiley-Interscience: New York, 1976.

(25) Nagao, H.; Aoyagi, K.; Yukawa, Y.; Howell, F. S.; Mukaida, M.; Kakihana, H. *Bull. Chem. Soc. Jpn.* **1987**, *60*, 3247.

(26) A solution of *trans*-$Ru(CN)_2(py)_4 \cdot H_2O$ (100 mg, 0.21 mmol) and LiCl (479 mg, 11.3 mmol) in pyridine (10 mL) and water (3 mL) was heated at reflux for 2 h. The yellow solution was concentrated to *ca.* 0.5 mL and water (20 mL) was added. The precipitate was collected by filtration, washed with water and dried to yield unreacted *trans*-$Ru(CN)_2(py)_4 \cdot H_2O$ (60 mg); δ_H ($CDCl_3$) 8.77 (8 H, d, $H^{2,6} \times 4$), 7.59 (4 H, t, $H^4 \times 4$), 7.07 (8 H, t, $H^{3,5} \times 4$). The yellow filtrate solution contained only further dicyano complex as evidenced by infrared spectroscopy.

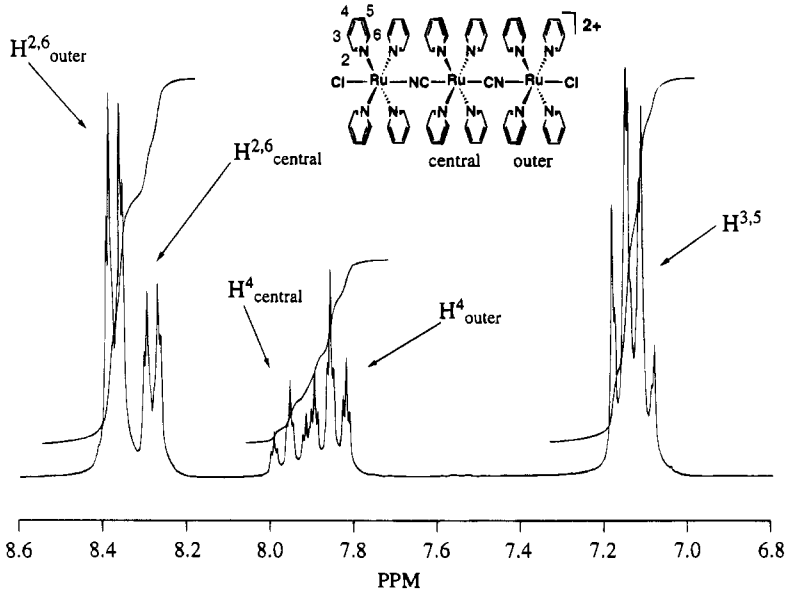

Figure 1. 200 MHz ^{1}H NMR spectrum of **2** in acetone-d_6 vs TMS.

indicating strong Ru−C bonding in the *trans*-dicyano unit, consistent with crystallographic studies (*vide infra*).

The PF_6^- salts **1**−**3** are all highly soluble in acetone or acetonitrile, but totally insoluble in water. The syntheses of these novel complexes are shown in Scheme 2.

^{1}H NMR Studies. The high symmetry of *trans*-$\{Ru(py)_4\}^{2+}$ complexes leads to simplified ^{1}H NMR spectra which are a valuable characterization tool. In the dimer **1** the two inequivalent metal centers give overlapping pyridine proton multiplets. In the trimer **2** the magnetic environments of the central and outer *trans*-$\{Ru(py)_4\}^{2+}$ units are sufficiently different for resolution of both the $H^{2,6}$ "doublets" and the H^4 "triplets". For the outer pyridines, this arises from a deshielding of the $H^{2,6}$ "doublets" but a shielding of the H^4 "triplets" with respect to those of the central pyridines (Figure 1). Replacement of the chloride ligands in **2** with acetonitrile to give **3** alters this pattern. In **3**, all 24 2,6-protons appear as a single "doublet". The H^4 "triplets" are overlapping, while the $H^{3,5}$ "triplets" are resolved, the pyridine protons of the central Ru center being shielded with respect to their peripheral counterparts.

FAB Mass Spectrometric Studies. The two trimetallic salts **2** and **3** were investigated by FAB mass spectrometry. For **2** the cation resulting from loss of one PF_6^- counterion ($[M - PF_6^-]$) is detected at an *m/z* ratio of 1524. The species resulting from loss of both counterions ($[M - 2PF_6^-])^{2+}$ is also detected at *m/z* 1379. Another particularly intense peak is found at *m/z* 923 corresponding to the fragment *trans*-$[Cl(py)_4Ru^{II}(NC)Ru^{II}(py)_4(CN)]^+$. Numerous smaller fragments are also detected. Similar behavior has been observed for other cyano-bridged polynuclear Ru complex salts.[27] The spectrum for **3** obtained under the same conditions is composed of too many peaks to yield any useful structural information.

Infrared Studies. Comparison with infrared spectra of related complexes is especially helpful in the characterization of *trans*-$[Ru(OCH_3)_2(py)_4]PF_6$. The closely similar complex *trans*-$[RuCl(OCH_3)(py)_4]^+$ has methoxy C−H stretching bands at 2860 and 2786 cm^{-1}, a methoxy C−O stretch at 1035 cm^{-1}, and a Ru−O stretch at 549 cm^{-1}.[25] The symmetrical bis(methoxy) complex $Mn(TPP)(OCH_3)_2$ (TPP = 5,10,15,20-tetraphenylporphinato) has three C−H stretches at 2888, 2855, and 2775 cm^{-1} and a C−O stretch at 1050 cm^{-1}.[28]

The most informative aspect of the infrared spectra of the new cyanide complexes is their cyanide stretching frequencies. Bridging cyanide frequencies (ν(CN*b*)) in polynuclear complexes are generally observed to high frequency of those of terminal cyanides (ν(CN*t*)).[1,29] This is attributed largely to kinematic coupling whereby the motion of the bridging CN is constrained by the second metal center.[29a] Very recent studies on cyano-bridged polypyridine complexes of Ru and other transition metals reveal that π back-bonding effects can also contribute markedly to the observed frequency shifts.[10] Back-bonding from the C-bonded metal is often important and is expected to be enhanced by the withdrawal of charge from the CN, which results from bridge formation. This will lead to a weakening of the C−N bond and hence a shift to lower frequency for ν(CN*b*). Back-bonding from the N-bonded metal may also be significant, acting to further lower ν(CN*b*).

The parent *trans*-$Ru(CN)_2(py)_4$ has a single, extremely intense ν(CN*t*) band at 2062 cm^{-1},[19] due to the antisymmetrical stretching of the two linearly bound *trans* cyanide ligands. Identical ν(CN*t*) bands are observed in the related complexes *trans*-$Ru(CN)_2(bpy)_2$,[17] and *trans*-$Ru(CN)_2(eda)_2$ (eda = ethylene-1,2-bis(diphenylarsine)).[30] Binding a *trans*-$\{RuCl(py)_4\}^+$ moiety to one of the cyanide nitrogens to form the dimer **1** breaks the symmetry of the complex. This would be expected to give rise to two bands for ν(CN*b*) and ν(CN*t*), as observed in *trans*-$(NC)Co(dppe)_2(CN)MX_3$ (dppe = 1,2-bis(diphenylphosphino)ethane; *e.g.*, M = Fe^{2+}, X = chloride).[31] However, the infrared spectrum of **1** has only a single cyanide stretching band at almost the same frequency as ν(CN*t*) for *trans*-$Ru(CN)_2(py)_4$, but of considerably lower intensity. Spectroscopic and electrochemical studies on the pyrazine-bridged complex $[\{trans\text{-}Ru^{II}Cl(py)_4\}_2(\mu\text{-pyz})]^{2+}$ have shown that the *trans*-$\{RuCl(py)_4\}^+$ center engages in extensive $d\pi(Ru^{II}) \rightarrow \pi^*$(pyz) back-donation,

(27) (a) Bignozzi, C. A.; Bortolini, O.; Traldi, P. *Rapid Commun. Mass Spectrom.* **1991**, *5*, 600. (b) Argazzi, R.; Bignozzi, C. A.; Bortolini, O.; Traldi, P. *Inorg. Chem.* **1993**, *32*, 1222.

(28) Camenzind, M. J.; Hollander, F. J.; Hill, C. L. *Inorg. Chem.* **1982**, *21*, 4301.

(29) (a) Dows, D. A.; Haim, A.; Wilmarth, W. K. *J. Inorg. Nucl. Chem.* **1961**, *21*, 33. (b) Shriver, D. F. *J. Am. Chem. Soc.* **1963**, *85*, 1405. (c) Alvarez, S.; López, C.; Bermejo, M. J. *Transition Met. Chem. (London)* **1984**, *9*, 123.

(30) Poddar, R. K.; Agarwala, U.; Manoharan, P. T. *J. Inorg. Nucl. Chem.* **1974**, *36*, 2275.

(31) Rigo, P.; Longato, B.; Favero, G. *Inorg. Chem.* **1972**, *11*, 300.

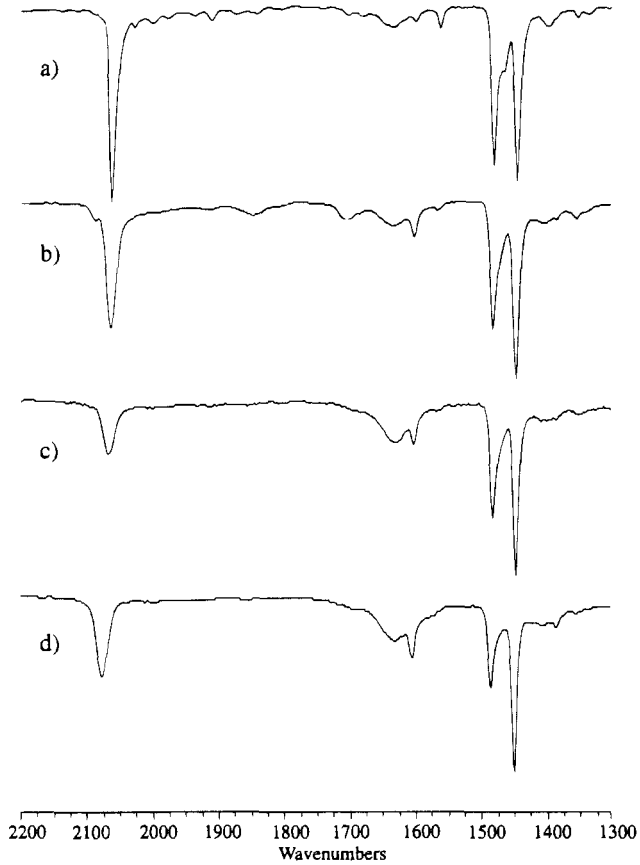

Figure 2. Infrared spectra (KBr disks) of *trans*-$Ru(CN)_2(py)_4$ (a), **1** (b), **2** (c), and **3** (d) in the region 2200−1300 cm^{-1}.

largely as a result of the relatively strong σ-donating character of the *trans* chloride ligands.[19] It appears that back-bonding from the N-bonded Ru, possibly accompanied by increased back-bonding from the C-bonded Ru, effectively counterbalances the kinematic effect in **1**, resulting in only a very slight change in ν(CN*b*) with respect to ν(CN*t*). The reduction in intensity is due to a decrease in the magnitude of the dipole moment changes accompanying the C-N stretching vibrations.

The trimer **2** has a single ν(CN*b*) band which is only 5 cm^{-1} higher in frequency, but is much less intense, than ν(CN*t*) for *trans*-$Ru(CN)_2(py)_4$. Hence, the ν(CN*b*)-lowering effects of back-bonding in **2** do not totally cancel the expected frequency increase due to the kinematic effect. The further reduction in intensity is due to an added decrease in the magnitude of the dipole moment change upon vibration. That *trans*-$Ru(CN)_2(py)_4$, **1**, and **2** all have similar ν(CN) frequencies is good evidence that no linkage isomerism is occurring. Substitution of the chlorides in **2** by acetonitrile to give **3** shifts ν(CN*b*) to high frequency by *ca.* 10 cm^{-1} (and 15 cm^{-1} higher than ν(CN*t*) for *trans*-$Ru(CN)_2(py)_4$), with a significant increase in intensity. This is due to a reduction in back-bonding from the N-bonded metals upon replacement of the relatively strong σ-donating *trans* chlorides with π-accepting acetonitriles, allowing the kinematic effect on ν(CN*b*) to predominate. Evidence for back-bonding from both C- and N-bonded Ru centers in **2** is seen in the bond lengths obtained from X-ray crystallography (*vide infra*).

Infrared spectra of *trans*-$Ru(CN)_2(py)_4$, **1**, **2**, and **3** are shown in Figure 2. The bands at *ca.* 1480 and 1445 cm^{-1} are found in all *trans*-$\{Ru(py)_4\}^{2+}$ complexes, and are assigned to the ν19a and ν19b vibrational modes of the coordinated pyridines.[32]

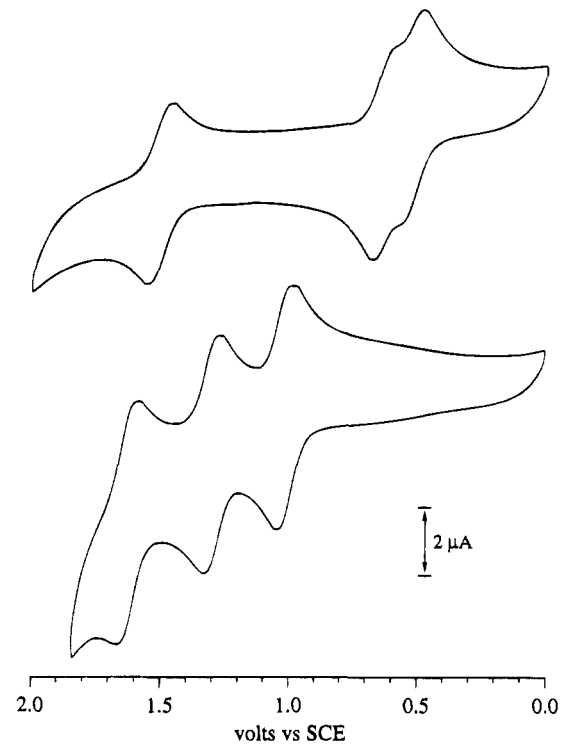

Figure 3. Cyclic voltammograms of **2** (upper) and **3** (lower) in acetonitrile 0.1 M in $[N(C_4H_9\text{-}n)_4]PF_6$ at 200 mV s^{-1}. Concentrations *ca.* 5 × 10^{-4} M (but not identical).

UV−Visible Studies. Absorption spectra for the new complexes were recorded in acetonitrile, and results are presented in Table 1. The Ru(II) complexes all show intense, broad $d\pi(Ru^{II}) \rightarrow \pi^*$(py) (MLCT) bands in the region 300−420 nm.[19,32] For *trans*-$[Ru(OCH_3)_2(py)_4]PF_6$, two $CH_3O^- \rightarrow Ru^{III}$ LMCT bands are observed at 316 and 416 nm. The related complex *trans*-$[RuCl(OCH_3)(py)_4]^+$ has bands at 301 and 427 nm with extinctions of 12 000 and 2300 M^{-1} cm^{-1} respectively.[25]

For the cyano-bridged salts **1** and **2** the $Ru^{II} \rightarrow$ py MLCT bands are similar in shape, and have maxima at almost the same wavelength, as that of *trans*-$Ru(CN)_2(py)_4$. There is an expected increase in extinction on binding first one (in **1**) and then two (in **2**) *trans*-$\{Ru(py)_4Cl\}^+$ moieties to the cyanide nitrogens because of the increased number of pyridine ligands. This is accompanied by an intensifying yellow coloration due to increased tailing of the MLCT band into the visible. In *trans*-$Ru(CN)_2(py)_4$ the extinction at 430 nm is 2200 M^{-1} cm^{-1}, in **1** this increases to 8000 M^{-1} cm^{-1}, and in **2** it is as high as 12 300 M^{-1} cm^{-1}. The complex in **3** is almost colorless, having a very intense $d\pi(Ru^{II}) \rightarrow \pi^*$(py) MLCT absorption at 346 nm, blue shifted by 24 nm with respect to that of its chloro precursor **2**. This is indicative of a raising in energy of the π^* LUMO of the pyridine ligands or, more likely, stabilization of the Ru $d\pi$ orbitals upon replacement of the chlorides by acetonitrile. The molar extinction coefficient per pyridine at the MLCT maximum remains nearly constant at 4500−5500 M^{-1} cm^{-1}.

In addition to the Ru → py MLCT bands, all of the complexes also show two or more high energy bands which are likely due to $\pi\pi^*$ excitations in the pyridine ligands. Intense $d\pi(Ru^{II}) \rightarrow \pi^*$(CN) MLCT absorptions are expected to occur at very high energy (< 200 nm), since those of $[Ru(CN)_6]^{4-}$ are found at 52 000 and 48 500 cm^{-1} (192 and 206 nm) in water.[33]

(32) Templeton, J. L. *J. Am. Chem. Soc.* **1979**, *101*, 4906.

(33) Seddon, E. A.; Seddon, K. *The Chemistry of Ruthenium*; Elsevier: Amsterdam, 1984; p 669.

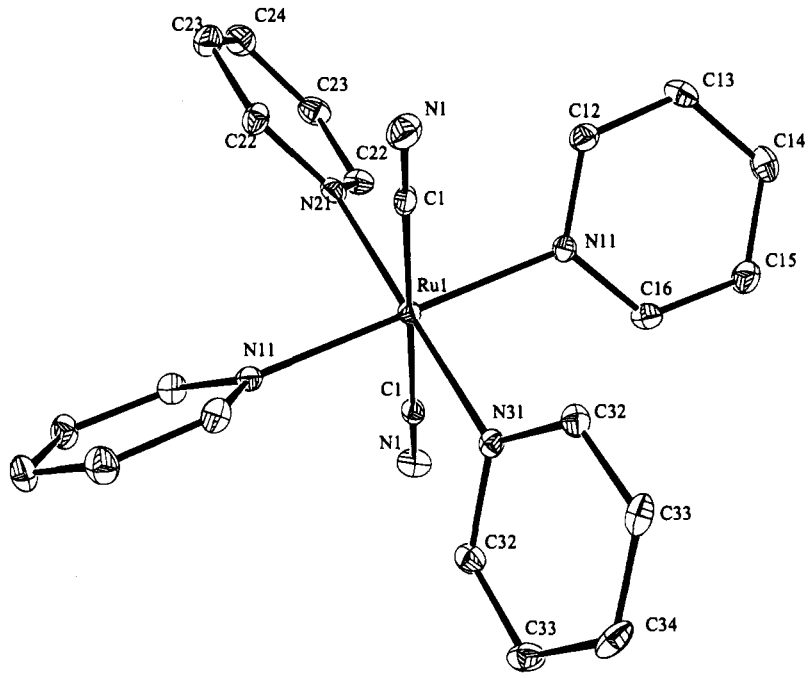

Figure 4. Structural representation of *trans*-$Ru(CN)_2(py)_4$, with hydrogen atoms omitted. The thermal ellipsoids correspond to 50% probability.

Electrochemical Studies. The electrochemical properties of the complexes were studied by cyclic voltammetry in acetonitrile, and results are given in Table 1. The complex *trans*-$[Ru(OCH_3)_2(py)_4]^+$ shows a reversible one-electron wave, assigned to the $Ru^{III/II}$ couple, at the highly cathodic potential of −0.82 V vs SCE. This compares with a value of −0.34 V for the *trans*-$[RuCl(OCH_3)(py)_4]^{+/0}$ couple in acetonitrile.[25] Substitution of chloride by methoxide is expected to produce a marked negative shift in reduction potential. A completely irreversible wave is observed at E_{pa} = 0.74 V vs SCE.

The bimetallic complex *trans*-$[Cl(py)_4Ru^{II}(NC)Ru^{II}(py)_4(CN)]^+$ (in **1**) shows two well separated, reversible $Ru^{III/II}$ oxidation waves. The wave at 0.53 V vs SCE corresponds to the $Ru^{III/II}$ couple of the chloride-bearing Ru center, shifted by +270 mV from that of *trans*-$RuCl_2(py)_4$[19] by binding to the mildly π-accepting N-terminus of the bridging cyanide. The wave at 1.20 V vs SCE is due to oxidation of the dicyano-substituted Ru center, the couple for which is shifted by +400 mV from that of *trans*-$Ru(CN)_2(py)_4$.

For the trimetallic complex *trans*-$[Cl(py)_4Ru^{II}(NC)Ru^{II}(py)_4(CN)Ru^{II}(py)_4Cl]^{2+}$ (in **2**), the outer Ru centers give two closely-spaced one-electron oxidation waves at 0.64 and 0.54 V vs SCE. The $\Delta E_{1/2}$ value of *ca.* 100 mV for these $Ru^{III/II}$ couples indicates a significant electronic coupling between the two metal centers, occurring via the bridging *trans*-$Ru(CN)_2(py)_4$ "ligand". The central Ru in **2** is oxidized at the highly positive potential of 1.51 V vs SCE which is a shift of +710 mV from the $Ru^{III/II}$ oxidation in *trans*-$Ru(CN)_2(py)_4$, and +310 mV from that in **1**.

Substitution of the chlorides in **2** by acetonitrile to give **3** has a dramatic effect on the electrochemical behavior of the linear trimetallic cyano-bridged unit. The $Ru^{III/II}$ oxidations for the outer Ru centers shift to much more positive potentials as a result of replacing the good σ-donor chloride by the moderate π-acceptor acetonitrile. Furthermore, and more remarkably, the electronic coupling between these Ru centers is greatly increased, as evidenced by a $\Delta E_{1/2}$ value of 280 mVfor **3**.[34] This substitution is expected to reduce $d\pi(Ru^{II}) \rightarrow \pi^*(CN)$ back-bonding, in accord with infrared studies (*vide supra*). Hence, the extensive coupling observed in **3** must result from electronic communication via the π, rather than the π^*, system of the Ru−NC−Ru−CN−Ru backbone. The central Ru in **3** is oxidized at 1.65 V vs SCE which is 140 mV positive of that for **2**. Cyclic voltammograms for **2** and **3** are shown in Figure 3.

Structural Studies. To our knowledge, the salt **2** contains the first example of a cyano-bridged triruthenium complex to be structurally characterized. There are a small number of reports of trinuclear Ru complexes featuring a *trans* geometry at the central metal. These include polynuclear pyrazine-bridged complexes based on the *trans*-$\{Ru(NH_3)_4\}^{2+}$ center,[35] and an oxo-bridged tris-$\{Ru(bpy)_2\}$ species which was assigned a structure containing a central *trans*-$\{Ru^{IV}(O)_2(bpy)_2\}$ unit on the basis of electrochemical studies.[36] The oxo-bridged trimetallic *trans* complex, ruthenium red, *trans*-$[(NH_3)_5Ru^{III}ORu^{IV}(NH_3)_4ORu^{III}(NH_3)_5]^{6+}$,[37] and also its ethylene diamine analogue[38] have been characterized by single-crystal X-ray diffraction.

Except for many polymeric complexes,[39] and some cluster compounds,[40] there are few X-ray structural reports of cyano-bridged complexes containing more than two metals. Two examples are the heterotrimetallic complexes *cis*-$[Ru^{II}(bpy)_2\{trans\text{-}Cr^{III}(cyclam)(CN)_2\}_2]^{4+}$,[6c] and *trans*-$[(CN)_5Fe^{II}(CN)Pt^{IV}(NH_3)_4(NC)Fe^{II}(CN)_5]^{4-}$.[7a]

The structure of *trans*-$Ru(CN)_2(py)_4$ is shown in Figure 4. The complex has the typical propeller formation of the *trans*-$\{Ru(py)_4\}^{2+}$ moiety,[19] with an uneven pitch of the pyridine rings.[41] The *trans*-$\{Ru(CN)_2\}$ unit is perfectly linear with bond angles C(1)−Ru(1)−C(1)a and Ru(1)−C(1)−N(1) of 179.92-

(34) The electrochemical behavior of **3** could be explained by invoking an asymmetrical linkage isomerized structure, *trans*-$[(MeCN)(py)_4Ru^{II}(CN)Ru^{II}(py)_4(CN)Ru^{II}(py)_4(MeCN)]^{4+}$, containing three inequivalent Ru(II) centers. However, this appears highly unlikely in the light of infrared, ^1H NMR, and synthetic observations.

(35) von Kameke, A.; Tom, G. M.; Taube, H. *Inorg. Chem.* **1978**, *17*, 1790.
(36) Geselowitz, D. A.; Kutner, W.; Meyer, T. J. *Inorg. Chem.* **1986**, *25*, 2015.
(37) de C. T. Carrondo, M. A. A. F.; Griffith, W. P.; Hall, J. P.; Skapski, A. C. *Biochim. Biophys. Acta* **1980**, *627*, 332.
(38) Smith, P. M.; Fealey, T.; Earley, J. E.; Silverton, J. V. *Inorg. Chem.* **1971**, *10*, 1943.
(39) (a) Shriver, D. F. *Struct. Bonding (Berlin)* **1966**, *1*, 32. (b) Ludi, A.; Güdel, H. U. *Struct. Bonding (Berlin)* **1973**, *14*, 1.
(40) See for example: Johnston, D. H.; Stern, C. L.; Shriver, D. F. *Inorg. Chem.* **1993**, *32*, 5170 and references therein.

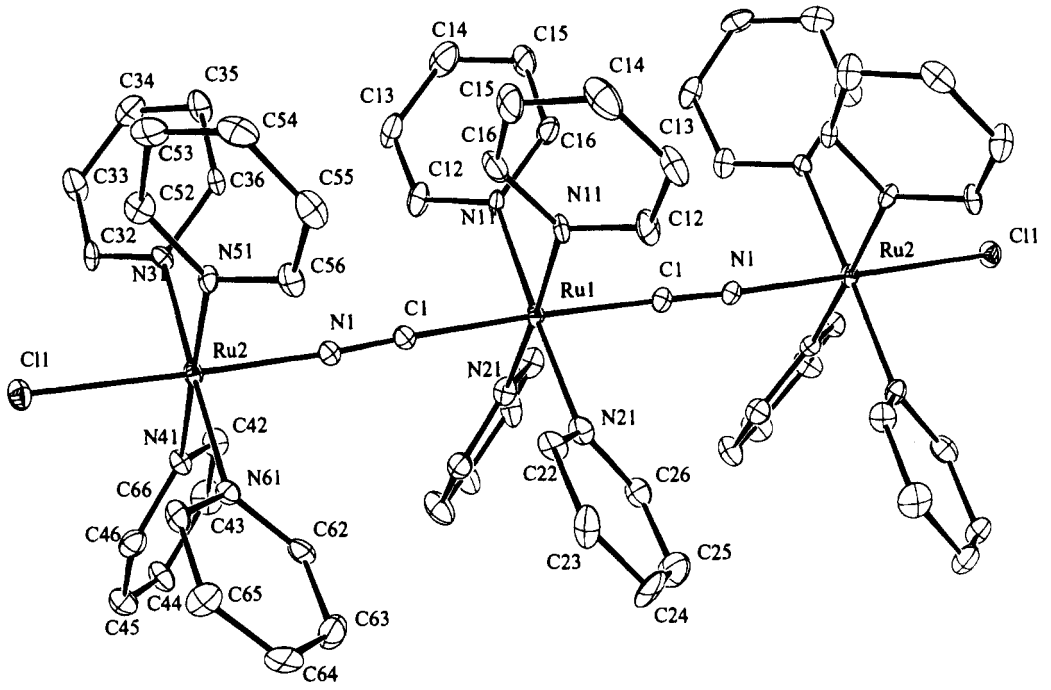

Figure 5. Structural representation of the cation of **2**, *trans*-$[Cl(py)_4Ru(NC)Ru(py)_4(CN)Ru(py)_4Cl]^{2+}$, with hydrogen atoms omitted. The thermal ellipsoids correspond to 50% probability.

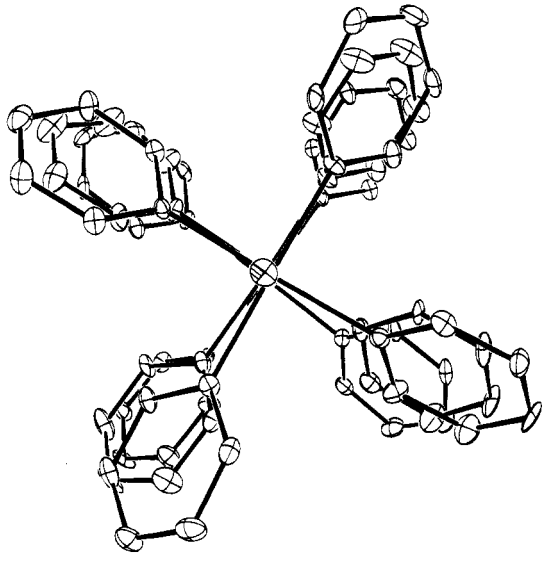

Figure 6. Alternate view of the cation of **2**, *trans*-$[Cl(py)_4Ru(NC)Ru(py)_4(CN)Ru(py)_4Cl]^{2+}$, along the Cl–Ru–NC–Ru–CN–Ru–Cl axis.

(21) and 179.4(3)°, respectively. The bond lengths Ru–C(cyanide) and C–N(cyanide) of 2.057(4) and 1.156(5) Å, respectively, are similar to those found in the mononuclear Ru(II) complex $[Ru(CN)_5(NO)]^{2-}$. As its hydrated sodium salt, the latter has average bond lengths for Ru–C and C–N (*trans* to CN) of 2.059(3) and 1.147(4) Å, respectively.[42] The Ru–C bonds are shortened by π back-bonding.

The structure of the cation in **2** is shown in Figure 5 with an alternate view shown in Figure 6. Since the C and N atoms cannot be distinguished on pure refinement grounds, the arrangement of the cyanide bridges depicted is that dictated by the synthetic procedure used, assuming no linkage isomerization (*vide supra*). The complex has an almost perfectly linear geometry with bond angles Cl(1)–Ru(2)–N(1), Ru(2)–N(1)–C(1), Ru(1)–C(1)–N(1), and C(1)–Ru(1)–C(1)a of 177.59(21), 176.6(9), 177.8(9), and 177.6(5)°, respectively. All three metal centers display the characteristic *trans*-$\{Ru(py)_4\}^{2+}$ propeller geometry,[19] with typical pitches,[43] and adopt an almost completely eclipsed configuration, as shown in Figure 6. Such an arrangement is also found in the pyrazine-bridged dimer $[\{trans\text{-}Ru^{II}Cl(py)_4\}_2(\mu\text{-pyz})]^{2+}$.[19] This geometry is required for the extensive π-overlap along the Ru–NC–Ru–CN–Ru backbone demonstrated by electrochemical studies (*vide supra*).

The Ru–C(cyanide) bond length of 2.040(10) Å is similar to those reported in $Mn_2[Ru(CN)_6]\cdot 8H_2O$ (average Ru–C distance = 2.028(6) Å),[44] and in the diruthenium complex $[(Cp)(dppe)Ru^{II}(CN)Ru^{II}(Cp)(PPh_3)_2]^+$ (Cp = η^5-cyclopentadienyl, Ru–C distance = 2.03(2) Å).[45] Although this bond is apparantly a little shorter than that in *trans*-$Ru(CN)_2(py)_4$, this difference may not be significant owing to the relatively large esd's. The Ru–N(cyanide) bond length of 2.013(8) Å is shorter than that in $[(Cp)(dppe)Ru^{II}(CN)Ru^{II}(Cp)(PPh_3)_2]^+$ (Ru–N distance = 2.07(1) Å),[45] but similar to that in *trans*-$[Ru^{II}Cl(py)_4(PhCN)]^+$ (PhCN = benzonitrile, Ru–N distance = 1.989(7) Å).[19] These bond lengths indicate $d\pi(Ru^{II}) \rightarrow \pi^*(CN)$ back-donation from both C- and N-bonded Ru centers, as suggested by infrared studies (*vide supra*), with a greater extent of back-bonding from the N-bound Ru centers.

The C–N bond length in the cyanide bridge is typical at 1.157(12) Å, and unchanged from that in *trans*-$Ru(CN)_2(py)_4$. C–N bond lengths of 1.160(8) Å (average) and 1.14(2) Å were found in $Mn_2[Ru(CN)_6]\cdot 8H_2O$,[44] and $[(Cp)(dppe)Ru^{II}(CN)Ru^{II}(Cp)(PPh_3)_2]^+$,[45] respectively. The Ru–Cl bond length is comparatively long at 2.4212(24) Å. A shorter bond length of

(41) Torsion angles for *trans*-$Ru(CN)_2(py)_4$ are as follows: Cl(1)–Ru(1)–N(11)–C(16) = −46.2(3)°; C(1)–Ru(1)–N(21)–C(22) = −34.6(3)°; C(1)–Ru(1)–N(31)–C(32) = 145.4(4)°.

(42) Olabe, J. A.; Gentil, L. A.; Rigotti, G.; Navaza, A. *Inorg. Chem.* **1984**, *23*, 4297.

(43) Torsion angles for **2** are as follows: Cl(1)–Ru(2)–N(31)–C(32) = −40.6(9)°; Cl(1)–Ru(2)–N(41)–C(46) = −45.1(9)°; Cl(1)–Ru(2)–N(51)–C(52) = −42.0(9)°; Cl(1)–Ru(2)–N(61)–C(66) = −37.5(9)°; C(1)–Ru(1)–N(11)–C(16) = −38.9(10)°; C(1)–Ru(1)–N(21)–C(22) = −45.0(10)°.

(44) Rüegg, M.; Ludi, A.; Rieder, K. *Inorg. Chem.* **1971**, *10*, 1773.

(45) Baird, G. J.; Davies, S. G.; Moon, S. D.; Simpson, S. J.; Jones, R. H. *J. Chem. Soc., Dalton Trans.* **1985**, 1479.

2.3931(22) Å was found in *trans*-$[Ru^{II}Cl(py)_4(PhCN)]^+$,[19] indicating that the *trans* influence of the *trans*-$Ru(CN)_2(py)_4$ "pseudonitrile ligand" is slightly greater than that of benzonitrile. This suggests that *trans*-$Ru(CN)_2(py)_4$ is a better σ-donor, but a weaker π-acceptor than benzonitrile.

Conclusions

The complex *trans*-$Ru(CN)_2(py)_4$ can be used as a starting point for the stepwise construction of nonchromophoric Ru(II) *trans* assemblies by addition of *trans*-$\{RuCl(py)_4\}^+$ units. The terminal chloride ligands can be substituted, showing promise for extension in one dimension to polynuclear structures containing five or more metal ions. Such complexes are of interest as potential "molecular wires" to connect redox-active or photoactive metal centers. The mixed-valence properties of the oxidized forms of the new cyano-bridged complexes are currently under investigation, together with those of related complexes in which the N-termini of *trans*-$Ru(CN)_2(py)_4$ are capped by $\{Ru^{III}(NH_3)_5\}^{3+}$.

Acknowledgment. Support by the National Science Foundation (Grant CHE-8806664) is gratefully acknowledged. We thank Robert M. Leasure for assistance with preparing Figure 2.

Supplementary Material Available: Tables of hydrogen atomic parameters, bond distances and angles, and anisotropic thermal parameters for *trans*-$Ru(CN)_2(py)_4$ (Tables A–C) and **2** (Tables D–F) (13 pages). Ordering information is given on any current masthead page.

IC941265F